A Variable Shape and Variable Stiffness Controller for Haptic Virtual Interactions

Benjamin C. Mac Murray, Bryan N. Peele, Patricia Xu, Josef Spjut, Omer Shapira, David Luebke, Robert F. Shepherd

***Abstract*— This paper presents an entirely compliant controller handle for use in virtual and augmented reality environments. The controller handle transitions between two static states: a semi-rigid, large diameter state when pneumatically pressurized and a soft, compressible, smaller diameter state when depressurized. We integrated the controller with a modified version of NVIDIA's VR Funhouse employing the two controller states to simulate the physical feel of two virtual objects. We used finite element modeling to downselect an internal elastomer lattice within the controller that controls deformation upon inflation. Finally, we show an example of using the compliance of the handle as an interaction input by designing an algorithm to identify rapid compressions of the handle as a signal to swap objects in the virtual environment.**

I. Introduction

Virtual- (VR) and Augmented-Reality (AR) are becoming increasingly prevalent tools for simulation, training, and entertainment. While current systems excel at immersing the user visually and aurally in a simulated environment, haptic interactions are usually limited to rigid controllers that offer only vibrotactile feedback, or no feedback at all. Many technologies have shown promise towards providing interfaces capable of haptic interactions including ultrasonics [1], voice coils [2], electrovibration [3], and fluidic pressurization [4]. Among these, fluidic actuators are unique in providing both high displacements and high forces [5]. Building upon these benefits, fluidic actuators have been integrated within gloves [6], [7] designed to provide haptic feedback; however, challenges remain in designing a universally-fitting glove that incorporates powerful, yet lightweight and safe actuators. Aside from glove motifs, soft pneumatic devices have also been investigated as shape-changing user interfaces [8]–[10]. In this project, we aimed to combine the forceful actuation of pneumatically powered soft devices with a universal controller handle that can represent the physical properties of virtual objects by changing shape and stiffness (Fig. 1). The particular mode of interaction we use may be described as Dynamic Passive Haptic Feedback [11], meaning the shape and stiffness transition between stable states that are maintained for extended durations. We note that the feedback is both tactile and kinesthetic, as the controller's shape change expands across the user's fingertips while also pushing against and deforming in response to the user's grip.

Our choice to use compliant, pneumatic actuators provides several advantages to this study. Air powered actuators can undergo large deformations in short timespans [12] while having a lightweight structure. Compressed air can also provide forceful actuation from readily available sources (e.g., compressors or storage canisters). Recent studies have shown methods to program the deformation of compliant, pneumatic systems; these methods, however, are limited to 2D deformation from 1D actuators [13] and 3D deformation from 2D actuators [14]. Here we seek to explore a foundation for programming 3D deformation from 3D actuators.

II. Design and Fabrication

A. Material Selection

To fabricate the 3D actuators, we chose to use a commercially available stereolithography printer (Carbon M1). To print the components, we selected their EPU-40 and RPU-70 materials. EPU-40 is an elastomeric polyurethane resin that exhibits both high compliance and high ultimate elongation; both of these properties are essential for the highly deformable structures designed in this work. After printing, we post-processed all EPU-40 and RPU-70 components using the following procedure: We rinsed all parts briefly with isopropyl alcohol and used pressurized air to remove residual resin from internal chambers, then applied uncured, unprinted resin to close any open vent holes and placed the part in a UV chamber (ECE 5000 Flood, Dymax) to solidify the resin. Finally, we then thermally cured the parts in an oven for 8 hours at 120 °C.

B. Internal Lattice

We elected to integrate lattices into the controller's interior for three reasons. First, the internal lattice provides structural support to the inflation chambers. Though the lattice is composed of an elastomer, it is sufficiently stiff to retain the external chamber shape. Second, internal elastomeric lattices aid in the device's deflation rate by

*The work was supported by the National Science Foundation (Grant: CMMI-1745139) and the Office of Naval Research (Grant: N00014-17-1-2837)

B. C. Mac Murray, B. N. Peele, P. Xu, and R. F. Shepherd are with Cornell University, Ithaca, NY 14850 USA.

J. Spjut, O. Shapira, and D. Luebke are with NVIDIA, Santa Clara, CA 95050 USA.

All correspondence should be addressed to Robert F. Shepherd: phone: 607-255-8654 email: rfs247@cornell.edu

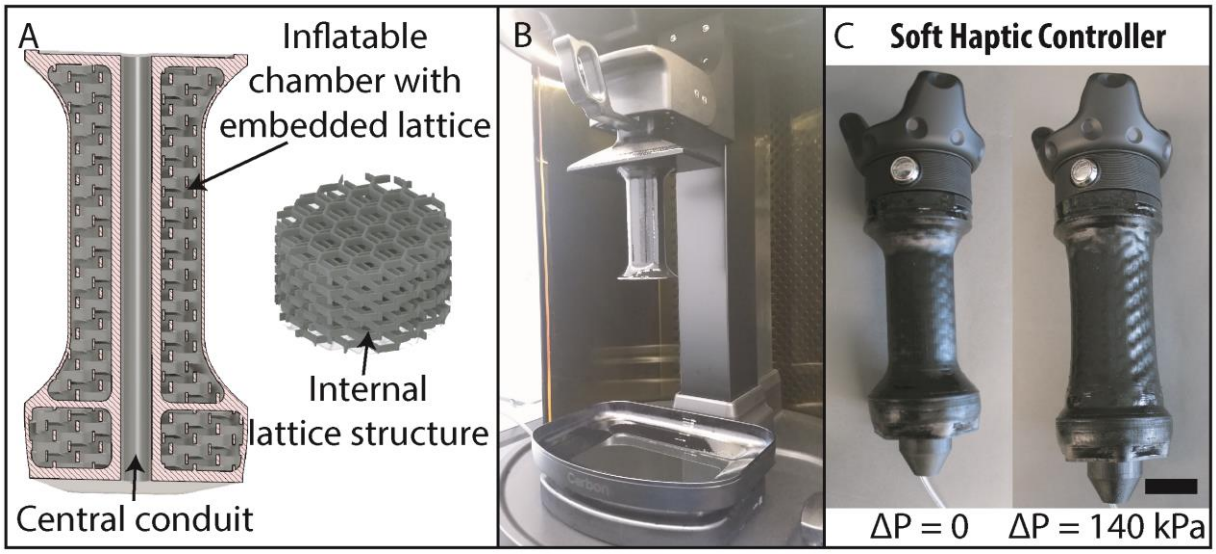

Figure 1: The compliant controller handle is composed of an internal elastomer lattice structure (A) and is printed via stereolithography (B). The handle expands from its unpressurized state (C, left) and increases stiffness when pressurized (C, right). Scale bar – 3 cm

providing an elastic restoring force towards the controller's uninflated shape. Finally, the lattices we chose provide an open, interconnected cellular network through the controller that enables resin flow during printing and air flow during actuation. Resin transport is important during printing as it reduces suction forces and trapped resin, both of which could lead to print failure.

To limit the search space for appropriate internal support structures, we used Bravais lattice geometries and modeled their deformation using finite element analysis (FEA). The lattices included simple cubic (*SC*), body-centered cubic (*BCC*), face-centered cubic (*FCC*), the union of BCC and FCC structures (*BCC + FCC*), and FCC without struts in the yz plane (*FCC no yz*). In addition to these base lattices, we also investigated a hexagonal honeycomb lattice structure.

C. Controller Handle

We designed the controller handle to be held with one hand and to have a dumbbell shape that curves around the user's fingers. A dumbbell shape creates an affordance that guides the user to wrap their fingers around the inner section of the device, where the interaction (and inflation) takes place. This affordance is meant to allow users to understand the shape of the device without seeing it, and to encourage them to readjust their grip during transitions between inflated/deflated states. The handle consists of an exterior skin and a central hollow cylindrical conduit (Fig. 1A) which are connected internally by the lattice. The cylindrical conduit enables wired connections to reach the button housing at the top of the controller.

The controller is composed of four components: (from the top of the controller, moving down to the handle base) the tracking device, the button housing, the inflatable handle, and the tether to the air source and control box (Fig. 2). We used a commercial Vive Tracker (HTC) that enables position/orientation tracking and simple integration with the HTC Vive VR setup. The button housing (Fig. 2A) served to provide both an interface between the Vive tracker and the handle and a rigid frame for the interactive button. The

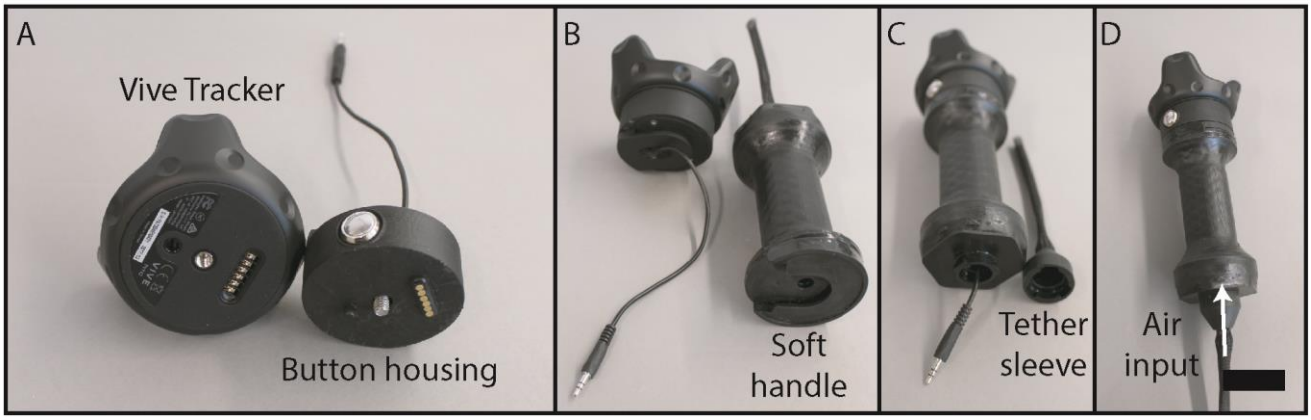

Figure 2: Modular assembly of the controller handle. (A) Our printed button housing connection to the Vive tracker, (B) the connection between the rigid button housing and the compliant handle, (C) the connection between the handle and the tether sleeve, and (D) the assembled controller. Scale bar – 6 cm

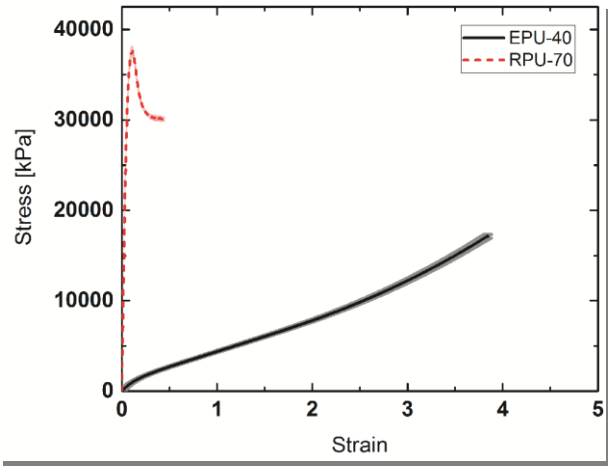

Figure 3: Stress-strain behavior of EPU-40 and RPU-70

interface between the Vive tracker and the housing consisted of a 6-pin electrical connection and a threaded screw connection (Fig. 2A). We designed the housing to be a hollow structure to contain the wires necessary for both the tracker and the button. The modularity of these components allowed for rapid iteration of controller handle designs.

III. Experimental Setup

We built digital models of each lattice in Solidworks 2017. The cubic lattices (simple, BCC, FCC, FCC no yz, and BCC+FCC) consist of 27 unit cells arranged in a 30x30x30 mm cube. These lattices are composed of struts with an octagonal cross-section with an edge to edge thickness of 1 mm. The simple lattice consisted of only vertical and horizontal struts, while the BCC and FCC structures had struts passing through their body diagonal and face diagonal, respectively. The hexagonal lattice is composed of a tessellated array of hollow hexagonal prisms with an edge to edge dimension of 12 mm, a thickness of 0.3 mm, and a height of 10 mm. We exported all digital models as .SAT file types to be imported into FEA software.

We used Static Structural analysis within Ansys Workbench 18.1 for all FE modeling. We imported the EPU 40 elastomer into the model as a 1st order Ogden material, as the Ogden model provided the best fit to our experimentally-measured uniaxial tensile data (Fig. 3). Ansys provided the fitting parameters of 1.4009E6 Pa, 2.4477, and 0 Pa^{-1} for Material Constant MU1, Material Constant A1, and Incompressibility Parameter D1, respectively, based on our imported tensile data. In the simulations, we meshed the lattices with an element size of 0.1 mm and enabled large deflections under Analysis Settings. We fixed the bottom lattice surface as a fixed support and applied tensile and compressive force to the top surface of each lattice. We measured the directional deformation response (in the direction parallel to loading) as the load was applied.

We performed all tensile tests according to ASTM D412 on a Zwick Roell z010 instrument. All tests used a 10 kN load cell and pulled at a strain rate of 10/min.

In order to integrate our custom controller with the application, we leveraged the HTC Vive tracker's integration with the SteamVR runtime. A firmware switch caused the tracker to appear as a normal controller to the application with full lighthouse-based tracking. NVIDIA's VR Funhouse was modified to send commands to a python script connected over a USB cable to an Arduino microcontroller that operated the valves. Furthermore, we added a virtual model of a foam sword using a soft-body physics simulation to the VR Funhouse environment.

IV. Results and Discussion

We used FEA to analyze several lattice geometries in compression and tension. While the relationship between stress and strain is often used to describe a material's tensile and compressive behavior, we intended to simulate a user applying a force to the controller's walls and then feeling a deformation. Because of this, we chose to observe the relationship between force and deformation directly in this study. A representative force vs. deformation plot is shown in Fig. 4 with accompanying images of the deformed lattice. We observe the deformation response to be linear under tensile loads and nonlinear under compressive loads. This loading (0.7 N) was sufficient to impart buckling of the lattice struts which forms the nonlinear behavior. When under compression, the lattice initially deforms linearly until it reaches a load of approximately 0.5 N. At this load, the struts begin to buckle and the lattice experiences large deformation with small increments in load. This behavior is consistent with compressive collapse of porous elastomers [15], [16].

We repeated this simulation with each lattice under forces from -0.01 N to 0.01 N, as shown in Fig. 5, and observed that each lattice deformed uniquely. In tension, all lattices demonstrated a largely linear response between deformation and force. Under compressive forces BCC, FCC no yz, and hexagonal lattices showed nonlinear behavior. This is due to the absence of struts parallel to the applied force in these lattices. The struts easily bend and buckle to allow large deformation under low forces.

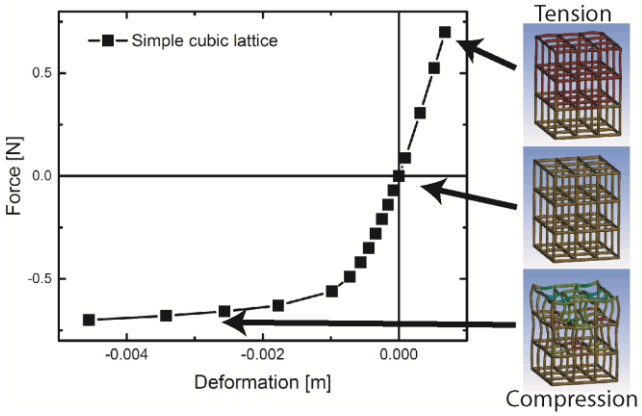

Figure 4: Representative simulated deformation of an elastomer lattice and the tensile and compressive simulated deformation of a simple cubic lattice. (from top to bottom) The simulated lattice shape at high tensile load, no load, and high compressive load.

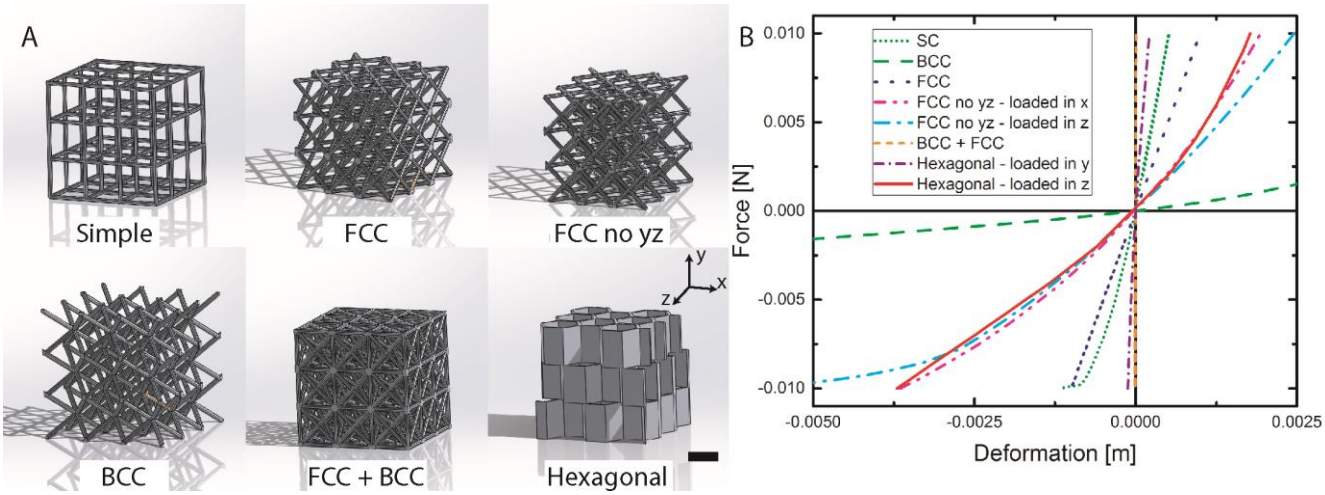

Figure 5: (A) The lattice models evaluated in this study and (B) their simulated tensile and compressive behavior. Scale bar – 10 mm

When designing the controller handle prototype, we made the internal structure a hexagonal honeycomb lattice. This structure was unique among those we examined in that it is largely radially symmetric (in the plane of the hexagons) and is relatively rigid in the perpendicular direction. This anisotropic behavior was oriented in the part to aid in printing the handle via stereolithography. That is, we aligned the stiff direction of the lattice with the build direction of the printer to reduce sagging during the print. This orientation of the lattice also allowed resin to drain easily as the part was drawn out of the printing resin.

We integrated the controller handle with a modified version of NVIDIA's VR Funhouse software (Supplemental Video). The demonstration consists of a single virtual environment where the user is surrounded by inflated balloons. The user initially interacts via a virtual metal sword which can pop the balloons. When using this sword, the controller handle is pressurized and increases its diameter and stiffness. With a keyboard or button press on the controller handle, the controller handle deflates to its highly compliant and reduced diameter state and the virtual object changes accordingly to a compliant, foam sword that is unable to pop balloons and instead bends when in contact with the balloons. The user can easily deform the handle by squeezing or bending in this state. The transitions between these states (e.g., inflating and deflating handle) occurs on the timescale of seconds in order to avoid potentially jolting rapid shape change. Inflation occurs over ~2 seconds and deflation occurs over ~7 seconds. These durations are dependent on the air source flow rate and the handle's air input diameter. Inflation/deflation could be increased and decreased by modifying these parameters.

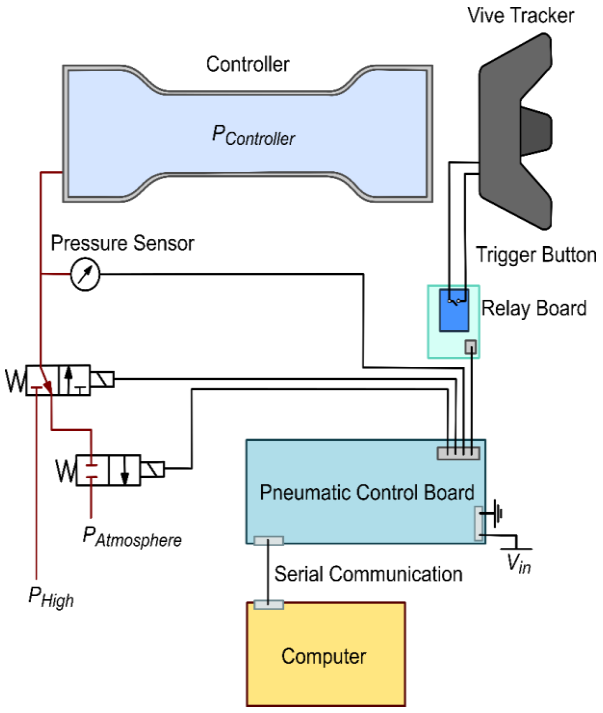

Figure 6: Controller prototype system integration schematic

The handle is controlled by a microcontroller (Arduino Uno) that integrates pneumatic valves (912-000001-031, Parker), a pneumatic pressure sensor (PSE530-R06, SMC Pneumatics), a relay (SRD-05VDC-SL-C, Songle), and the serial connection to a VR-ready computer (Fig. 6). The valves control the handle's internal air pressure by inflating from a pressure source (air compressor, model TC-848, TCP Global) or venting to atmosphere. The relay allowed an external button to trigger the transition between virtual objects.

We also demonstrated handle deformation as an input mechanism. Using real-time readings of the inline pressure sensor, we identified short duration pressure spikes (caused by the user squeezing the handle) as a signal to change objects in the virtual environment. Because we intended occasional deformation of the handle as part of normal handling, we wrote an algorithm to avoid false positives. This algorithm ignores isolated pressure spikes and identifies only two pressure spikes in quick succession as a signal to change the virtual object. A typical pressure profile showing this interaction is shown in Fig. 7.

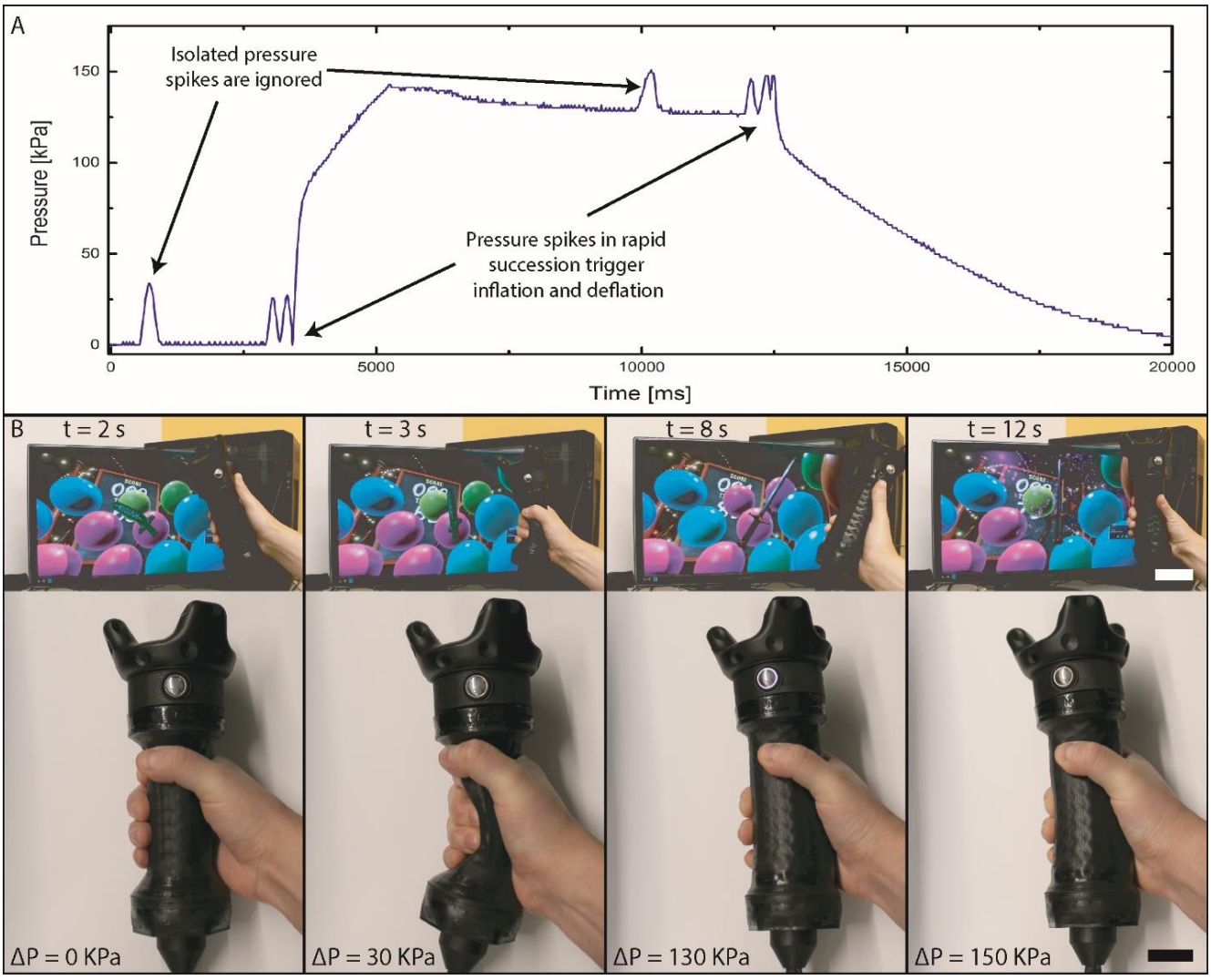

Figure 7: (A) Representative pressure profile of user-triggered inflation and deflation. (B) Sequence of demonstration interactions: [from left to right] interaction with a compliant handle corresponding to a virtual foam sword, rapid compressions of the unpressurized handle create successive pressure spike signaling to the controller to initiate a inflate the handle, interaction with the pressurized handle corresponding to a virtual metal sword, and successive compressions of the pressurized handle trigger deflation as the virtual object returns to a foam sword. Scale bars – 3 cm

Fig. 7 also shows the durations of inflation and deflation. The device inflates in ~2 seconds and deflates in ~ 7 seconds. We attribute the difference between inflation rate and deflation rate to different pressure differentials driving these processes. While we aimed for gradual inflation and deflation rates in this demonstration, future iterations could attain faster rates by using a wider diameter pneumatic input and output to increase air flow rates. Ultimately, this device's flow rates were limited by its 3 mm diameter pneumatic tubing.

V. Conclusions and Future Work

In this work, we investigated a foundation for designing and evaluating lattice-based pneumatic devices. We used FEA to evaluate several representative lattice structures in both tension and compression. Each lattice demonstrated unique behavior relative to the other structures. Lattices that contained struts which were easily bent and buckled contributed to more compliant behavior in compression. An expanded deformation map, including additional lattices and/or additional loading directions, could be used to design an internal lattice structure in which each unit cell dictates the local deformation at that point in 3D space, allowing fully programmable force/deformation properties.

We also designed and fabricated a controller handle for interaction with different virtual objects. While there are several haptic feedback devices available for computer interfaces, there are few that have been demonstrated, beyond vibrotactile, with the freedom of movement required for a VR environment. Our controller handle was based on an internal hexagonal lattice structure. The hexagonal structure provided the best compromise between comfortable squeezing of the controller and shape retention during inflation. As this controller is a human interface, it is a somewhat qualitative statement; further, quantitative, improvements will require topology optimization with a goal

of maximum shape retention upon pressurization and minimal stiffness when deflated.

Our controller handle switched between two states, pressurized and unpressurized, to simulate both a rigid and a compressible virtual object. To maintain control simplicity we decided to demonstrate the handle switching between only two states, however the system is also capable of continuous changes to shape and stiffness. Combined with a control system capable of maintaining air pressures along a continuum, this handle could provide a range of shape and stiffness change, approximating a wider range of virtual objects. This effort will require virtual objects that take advantage of the continuum and requires further investigation.

We used the compliance of the controller as a means of interaction. By squeezing in quick succession, the user was able to change the form of objects in the virtual environment and the stiffness and shape of the pneumatic controller.

While this handle design contained a single pneumatic chamber, future versions could contain multiple individually addressable chambers to simulate objects with more complex geometry and finer mapping to the human hand. With further refinement of the design, it may be possible to simulate changes in texture as well as changes in shape and stiffness.

ACKNOWLEDGMENT

B. C. M. thanks Rajesh Bhaskaran for assisting with Ansys.

REFERENCES

[1] F. Giraud, M. Amberg, and B. Lemaire-Semail, "Control of a haptic interface actuated by Ultrasonic Motors," *Proc. EPE-PEMC 2010 - 14th Int. Power Electron. Motion Control Conf.*, pp. 86–89, 2010.

[2] M. Gabardi, M. Solazzi, D. Leonardis, and A. Frisoli, "A new wearable fingertip haptic interface for the rendering of virtual shapes and surface features," *IEEE Haptics Symp. HAPTICS*, vol. 2016–April, pp. 140–146, 2016.

[3] O. Bau, I. Poupyrev, A. Israr, and C. Harrison, "TeslaTouch," *Proc. 23nd Annu. ACM Symp. User interface Softw. Technol. - UIST '10*, p. 283, 2010.

[4] C. Harrison and S. E. Hudson, "Providing dynamically changeable physical buttons on a visual display," *Proc. 27th Int. Conf. Hum. factors Comput. Syst. - CHI 09*, p. 299, 2009.

[5] N. Yu, C. Hollnagel, A. Blickenstorfer, S. Kollias, and R. Riener, "fMRI-Compatible Robotic Interfaces with Fluidic Actuation," *Robot. Sci. Syst.*, pp. 199–205, 2009.

[6] L. Connelly, Y. Jia, M. L. Toro, M. E. Stoykov, R. V. Kenyon, and D. G. Kamper, "A pneumatic glove and immersive virtual reality environment for hand rehabilitative training after stroke," *IEEE Trans. Neural Syst. Rehabil. Eng.*, vol. 18, no. 5, pp. 551–559, 2010.

[7] S. Jadhav, V. Kannanda, B. Kang, M. T. Tolley, and J. P. Schulze, "Soft robotic glove for kinesthetic haptic feedback in virtual reality environments," *IS&T Int. Symp. Electron. Imaging 2017*, pp. 19–24, 2017.

[8] L. Yao, R. Niiyama, and J. Ou, "PneUI: pneumatically actuated soft composite materials for shape changing interfaces," in *User interface software and Technology*, 2013.

[9] C. Larson, J. Spjut, R. Knepper, and R. Shepherd, "OrbTouch: Recognizing Human Touch in Deformable Interfaces with Deep Neural Networks," 2017.

[10] R. Shepherd, B. Peele, B. C. Mac Murray, J. Barreiros, O. Shapira, J. Spjut, and D. Luebke, "Stretchable Transducers for Kinesthetic Interactions in Virtual Reality," in *SIGGRAPH 2017 Emerging Technologies*, 2017.

[11] A. Zenner and A. Kruger, "Shifty: A Weight-Shifting Dynamic Passive Haptic Proxy to Enhance Object Perception in Virtual Reality," *IEEE Trans. Vis. Comput. Graph.*, vol. 23, no. 4, pp. 1312–1321, 2017.

[12] B. Mosadegh, P. Polygerinos, C. Keplinger, S. Wennstedt, R. F. Shepherd, U. Gupta, J. Shim, K. Bertoldi, C. J. Walsh, and G. M. Whitesides, "Pneumatic Networks for Soft Robotics that Actuate Rapidly," *Adv. Funct. Mater.*, vol. 24, no. 15, pp. 2163–2170, Dec. 2013.

[13] K. C. Galloway, P. Polygerinos, C. J. Walsh, and R. J. Wood, "Mechanically programmable bend radius for fiber-reinforced soft actuators," *2013 16th Int. Conf. Adv. Robot. ICAR 2013*, 2013.

[14] J. H. Pikul, S. Li, H. Bai, R. T. Hanlon, I. Cohen, and R. F. Shepherd, "Stretchable surfaces with programmable 3D texture morphing for synthetic camouflaging skins," *Science (80-.).*, vol. 358, no. 6360, pp. 210–214, 2017.

[15] J. A. Elliott, A. H. Windle, J. R. Hobdell, G. Eeckhaut, R. J. Oldman, W. Ludwig, E. Boller, P. Cloetens, and J. Baruchel, "In-situ deformation of an open-cell flexible polyurethane foam characterised by 3D computed microtomography," *J. Mater. Sci.*, vol. 37, no. 8, pp. 1547–1555, 2002.

[16] B. C. Mac Murray, C. C. Futran, J. Lee, K. W. O'Brien, A. A. Amiri Moghadam, B. Mosadegh, M. N. Silberstein, J. K. Min, and R. F. Shepherd, "Compliant Buckled Foam Actuators and Application in Patient-Specific Direct Cardiac Compression," *Soft Robot.*, vol. 0, no. 0, p. soro.2017.0018, 2017.